J. Fluid Mech. (1990), *vol.* 219, *pp.* 609–619
Printed in Great Britain

Waves from an oscillatory disturbance in a stratified shear flow

By R. LIU, D. NICOLAOU AND T. N. STEVENSON
Department of Engineering, University of Manchester, Oxford Road, Manchester M13 9PL, UK

(Received 29 November 1989)

It is shown how the St Andrew's cross-wave in a density-stratified fluid is modified by a horizontal shear above the level of the source. Ray theory is used to develop the equations for the phase configuration and it is shown that, for the special case when the background natural frequency is constant and the shear is linear, the wave crests are straight lines passing through the source. The waves corresponding to outgoing energy have phase velocities directed towards the horizontal level of the source and the waves which have undergone a reflection have phase velocities directed towards the vertical. It is shown that the ray theory predictions compare well with experiment and with finite-difference calculations.

1. Introduction

For a density-stratified fluid which has a constant natural frequency N and no mean flow, inviscid theory shows that energy propagating from an oscillatory source whose frequency ω is less than N propagates in straight lines at an angle $\sin^{-1}(\omega/N)$ to the horizontal forming a cross-wave in a vertical plane through the source. The wave crests lie along the cross-arms and the phase velocities are directed towards the level of the source. All wavenumbers propagate along the same ray lines. Mowbray & Rarity (1967) considered the far-field wave system. Appleby & Crighton (1986, 1987) considered an oscillating cylinder and an oscillating sphere in a stratified fluid. They matched an inner solution satisfying inviscid boundary conditions around the body with outer solutions which included non-Boussinesq terms.

Viscosity attenuates the velocities and increases the dispersion, widening the arms of the cross. The viscous non-Boussinesq similarity solution of Thomas & Stevenson (1972) is still essentially a St Andrew's cross-wave with straight arms, but any variation in the background natural frequency produces curvature in the cross-arms (Gordon, Klement & Stevenson 1975). In a fluid of constant natural frequency, a source oscillating at this frequency produces a strong vertical wave (Gordon & Stevenson 1972). In thermoclines or halines the energy reflects at caustics where the background natural frequency is equal to the source frequency, and the ray lines and the phase configuration have cusps as in figure 1.

When a shear flow is present, internal waves can reflect at caustics even when the background natural frequency is constant. In a thermocline with no shear the position of the caustic depends only on the wave frequency and the natural frequency distribution. However, in a shear flow it will also depend on the horizontal wavenumber and the shear velocity profile, and waves of different wavenumber will reflect at different altitudes. An important feature of stratified shear flows is the existence of critical levels where the frequency of oscillation relative to the fluid vanishes and the wave energy is transferred to the mean flow. A detailed study of

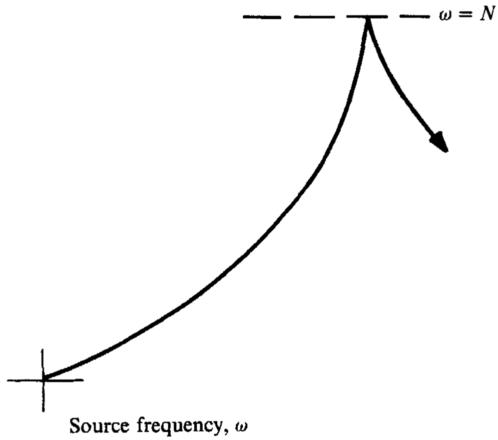

FIGURE 1. A wave reflection in a thermocline without a shear flow.

critical-layer absorptions of internal waves has been given by Booker & Bretherton (1967). Experimental investigations of viscous internal waves from moving bodies in stratified shear flows were presented by Koop (1981) and Koop & McGee (1986). They looked at the interaction of internal waves with the background shear near critical layers and presented a viscous wave action analysis based on the work of Grimshaw (1974) to predict wave amplitudes and the occurrence of wave overturning near the critical level.

In shear flows it is important to distinguish between the phase configuration and the ray paths relative to the fluid and relative to the source. There are misleading diagrams in the literature, e.g. Phillips (1966, p. 237, figure 5.16*a*) and Koop (1981, figure 8*c*), where there is no distinction between the phase configurations and the ray paths. The indications are that both should look like those in the unsheared thermocline, figure 1. This is not so.

In the next section the equations for internal waves generated by an oscillatory disturbance will be derived in terms of ray theory. In general they must be integrated numerically to obtain the ray paths and the phase configuration. An analytical solution is obtained for the special case when the shear is linear and the background natural frequency is constant. The waves for this case will be compared with experiment and with finite-difference calculations.

2. Ray tracing in a shear flow

Consider two-dimensional internal waves in a background flow in which the velocity in the $[x, z]$ direction is $[U(z), 0]$ where x is in a horizontal plane and z is measured vertically upwards. We make use of the WKB approximation and use ray theory together with the dispersion relation and the standard far-field expressions for the group velocity, which apply to a stable density-stratified fluid with constant natural frequency and no background shear, and apply these 'relative to the fluid' along ray lines in a fluid with a natural frequency $N(z)$ and with a background shear. The frequency relation (Bretherton 1966) is

$$\omega = \omega_r + kU, \tag{1}$$

where ω is the frequency of oscillation in a frame of reference fixed in space and ω_r

is the intrinsic frequency relative to the fluid and is related to the wavenumber vector $\boldsymbol{K} = [k, m]$ by

$$\omega_r^2 = \frac{N^2k^2}{k^2+m^2}. \tag{2}$$

The group velocity relative to the fluid is

$$\boldsymbol{c}_{gr} = [u_{gr}, w_{gr}] = \left[\frac{\partial \omega_r}{\partial k}, \frac{\partial \omega_r}{\partial m}\right] = \frac{N^2km}{\omega_r(k^2+m^2)^2}[m, -k]. \tag{3}$$

If $\theta(z)$ is the angle between the relative group velocity vector and the horizontal, then the wavenumber vector $\boldsymbol{K}$ makes an angle $\theta(z)$ with the vertical. If $\theta(z)$ is measured anticlockwise from the positive x-direction then ω_r and $\boldsymbol{c}_{gr}$ can be written as

$$\omega_r = N|\sin\theta| \tag{4}$$

and

$$\boldsymbol{c}_{gr} = [u_{gr}, w_{gr}] = \omega_r k^{-1}\cos\theta\sin\theta\,[\cot\theta, 1]. \tag{5}$$

Ray paths are defined by

$$\frac{dx}{dt} = u_g = U + u_{gr}, \quad \frac{dz}{dt} = w_g = w_{gr}, \tag{6}$$

so that

$$\frac{dx}{dz} = \frac{U+u_{gr}}{w_{gr}} = \frac{kU}{\omega_r\cos\theta\sin\theta} + \cot\theta. \tag{7}$$

As energy propagates along a ray path the frequency ω and the horizontal wavenumber k remain constant and the relative frequency ω_r and the vertical wavenumber m vary with z according to (1) and (2).

When internal waves are generated by a source of frequency ω, the phase of a wave group, $\phi = (kx+mz-\omega t)$, changes along the ray path at a rate of

$$\frac{d\phi}{dt} = \frac{\partial\phi}{\partial t} + \frac{\partial\phi}{\partial x}\frac{dx}{dt} + \frac{\partial\phi}{\partial z}\frac{dz}{dt} = -\omega + kU + \boldsymbol{K}\cdot\boldsymbol{c}_{gr}. \tag{8}$$

From (3)

$$\boldsymbol{K}\cdot\boldsymbol{c}_{gr} = 0, \quad \text{so that} \quad d\phi/dt = -\omega + kU. \tag{9}$$

Let the source be at the origin of the $[x, z]$ coordinate system. At time t_1 energy of frequency ω propagates away from the source along a ray path. At a later time t the energy will have reached a new position $[x, z]$ and have the phase

$$\phi = -\omega t_1 + \int_{t_1}^{t} d\phi + \Phi_R, \tag{10}$$

where $-\omega t_1$ is the phase of the source at time t_1. The integral represents the phase change that occurs as the energy propagates along the ray path during the time $(t-t_1)$ and Φ_R is the phase shift due to reflection at caustics where $\omega_r = N$. Actually, ray theory breaks down in the region near a caustic but it may be 'healed' in shear flows by a method similar to that used by Lighthill (1978) for the unsheared case. It is found that the phase change is $\frac{1}{2}\pi$ minus a small change due to any second gradient of the background shear velocity (Liu 1989). For a linear shear flow, i.e. one in which $U(z)$ varies as $Sz+U_0$ with S and U_0 constant, the phase shift is $\frac{1}{2}\pi$ as for the unsheared thermocline.

From the above equations it follows that

$$\phi = -\omega t + k\int_0^z \frac{\Omega - |\sin\theta|}{|\sin\theta|\sin\theta\cos\theta}dz + \Phi_R, \tag{11}$$

where $\Omega = \omega/N(z)$ and θ is related to z by the equation

$$N(z)\,|\sin\theta(z)| = \omega - kU(z). \tag{12}$$

Equations (11) and (12) can be used to compute phase configurations of the waves and (7) can be integrated to obtain the ray paths.

The radiation condition implies that $dt > 0$ or from (5) and (6)

$$\frac{k\,dz}{\omega_r\cos\theta\sin\theta} > 0 \quad \text{or simply} \quad \frac{k}{\cos\theta} > 0. \tag{13}$$

The permitted values of θ which determine the directions in which the energy can radiate from the source are those which satisfy both (12) and (13). The conditions combine to give

$$\frac{\Omega - |\sin\theta|}{U\cos\theta} > 0. \tag{14}$$

3. Waves in a uniformly stratified shear flow

The above analysis was for arbitrary distributions of $N(z)$ and $U(z)$. However, the equations can be integrated analytically when N is constant and U is a linear function of z,

$$U = Sz + U_0, \tag{15}$$

where S and U_0 are constants. From (12) and (15)

$$dz = -\frac{N\sin\theta\cos\theta\,d\theta}{Sk|\sin\theta|} \tag{16}$$

which is substituted into (7) to give

$$x = \frac{N}{Sk}\int_{\theta_1}^{\theta}\left\{|\sin\theta| - \frac{\Omega}{\sin^2\theta}\right\}d\theta, \tag{17}$$

where θ_1 is given by $N|\sin\theta_1| = \omega - kU_0$.

Equation (17) integrates to

$$x = N\frac{\cot\theta(\Omega - |\sin\theta|) - \cot\theta_1(\Omega - |\sin\theta_1|)}{Sk} \tag{18}$$

and from (12) and (15) the corresponding vertical coordinate is

$$z = N\frac{\Omega - |\sin\theta| - kU_0/N}{Sk}. \tag{19}$$

From (11) and (16)

$$\Phi = \frac{N}{S}\int_{\theta_1}^{\theta}\frac{(|\sin\theta| - \Omega)}{\sin^2\theta}d\theta + \Phi_R, \tag{20}$$

where $\Phi = \phi + \omega t$. For waves prior to reflection or for waves which will not reflect, this integrates to

$$\Phi = \frac{N}{S}\{\Omega(\cot\theta - \cot\theta_1) \pm \ln|\tan(\tfrac{1}{2}\theta)\cot(\tfrac{1}{2}\theta_1)|\} \tag{21}$$

and for reflected waves

$$\Phi = \frac{N}{S}\{\Omega(\cot\theta - \cot\theta_1) \mp \ln|\tan(\tfrac{1}{2}\theta)\tan(\tfrac{1}{2}\theta_1)|\} + \Phi_R, \tag{22}$$

where the upper sign is taken when $\sin\theta_1 > 0$.

4. The waves when $U_0 = 0$

$U_0 = 0$ corresponds to no background velocity at the level of the source or to a source moving with the background fluid at the level of the source. The phase configuration for this case can readily be deduced from the above equations. The equation

$$|\sin\theta_1| = \frac{\omega}{N} = \Omega = \text{constant} \tag{23}$$

determines four directions in which the energy generated by the source can propagate. It is seen from (21) and (22) that at any particular instant t, the lines of constant phase correspond to lines of constant θ. However, from (18) and (19), $z/x = \tan\theta$ which implies that lines of constant phase are straight lines emanating from the source at the origin, each line being inclined to the horizontal at the angle θ.

Regardless of k, equation (5) gives $w_{gr}/u_{gr} = \tan\theta$ so, since lines of constant phase are given by $z/x = \tan\theta = $ constant, the relative group velocity vector is always parallel to lines of constant phase as in the case when no shear is present. However, whilst energy is behaving relative to the fluid as if it were in a stationary fluid, it is at the same time being convected downstream by the local background flow. As energy moves from one level to another its frequency and vertical wavenumber change so that it behaves differently relative to the fluid at different levels. The overall effect is to produce ray and phase patterns which are distinctly different from each other.

The above results are illustrated in figure 2 for the case when $N = 1.3$ rad/s, $\omega = 0.785$ rad/s and $S = 0.04\ \text{s}^{-1}$. It is seen that the ray paths form two types of pattern. For energy propagating against the current the ray paths are a series of nested loops which have a common point at the origin. Relative to the fluid the ray paths are cusped at reflection. The position at which the energy reflects, from (18), (19) and (20) with $\theta = \tfrac{1}{2}\pi$ and $U_0 = 0$, is

$$(x, z) = (0, N(\Omega - 1)/Sk),$$

which shows that waves of all wavenumbers reflect on a vertical line passing through the body.

In figure 2 each ray path is for a different horizontal wavenumber k, the largest loops having the lowest values of k. Corresponding energy, that is energy which left the source at a particular instant, is found on a straight line from the source and all the energy has the same phase. Thus, all wavenumbers reach their farthest position from the source, where they reflect, at the same time. Corresponding energy propagating with the current behaves in a similar way except that it approaches critical levels where $\omega_r = 0$ instead of reflecting at caustics. In view of this, wave crests and troughs are straight lines.

The positions at which $\omega_r = 0$ are given by

$$(x, z) = (\pm\infty, \omega/Sk),$$

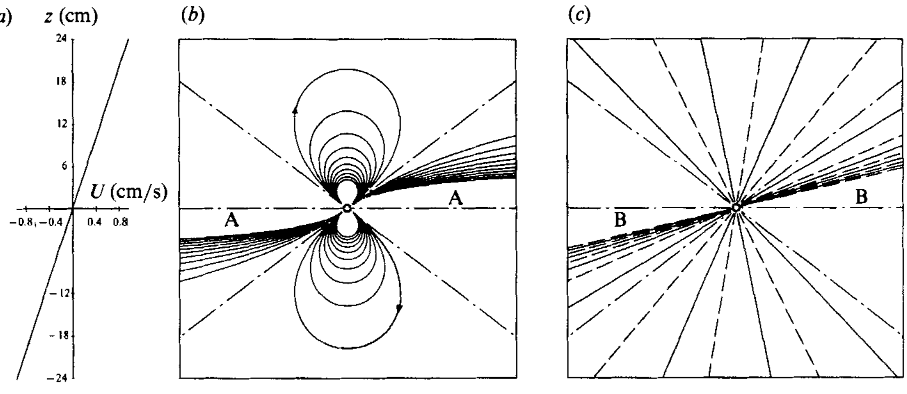

FIGURE 2. The cross-wave in a uniformly stratified linear shear layer. $N = 1.3$ rad/s, $\omega = 0.785$ rad/s. (*a*) Shear profile, $dU/dz = 0.04\ s^{-1}$. (*b*) Ray paths. (*c*) Phase configuration: the chain dotted line represents the cross-wave when shear is absent and neighbouring solid and dashed lines differ in phase by π. Regions A are filled with ray lines and sectors B with lines of constant phase.

so that again the lowest values of k travel to greatest heights. From (20) the angular phase velocity is

$$\frac{d\theta}{dt} = \omega\left\{\frac{d\Phi}{d\theta}\right\}^{-1} = \frac{S\sin^2\theta}{(|\sin\theta|/\Omega)-1}. \tag{24}$$

This equation shows that the crests and troughs of unreflected waves move towards the horizontal level of the source while those from reflected waves move towards the vertical. Thus, referring to figure 2(*c*), in the region above the source, wave crests emerge from the right-hand chain-dotted line, which is inclined to the horizontal at an angle $\sin^{-1}(\omega/N)$, and then move away from it.

5. Finite-difference calculations

Finite-difference calculations are used to support the analytical results and to illustrate the effects of viscosity and source width on the internal waves. The full Navier–Stokes equations are solved by the 'marker and cell' method for a stratified fluid (Young & Hirt 1972) with the open boundary conditions of Hirt & Cook (1972). Liu & Stevenson (1989) showed that the program agrees well with the viscous similarity solution for the St Andrew's cross-wave (Thomas & Stevenson 1972) for a stratified fluid with constant N and no shear.

Figure 3 shows a finite-difference solution of a viscous cross-wave in a uniformly stratified shear layer under the conditions of the analytical solution of figure 2. The waves are generated by a square body, with sides of 20 mm, in a domain of 96×96 square cells which have sides of 5 mm. The natural frequency, the wave frequency ω and the shear gradient S are the same as those in figure 2. Initially the body is at rest and the shear flow is such that the body is in a region of stationary fluid (see figure 3). A horizontal wake region develops on either side of the body during the computations. The body oscillates horizontally in simple harmonic motion with a maximum velocity of 0.785 mm/s. The viscosity μ is 0.001 N s/m^2. The velocity vector plot presented in figure 3(*b*) shows the perturbation velocity field and figure 3(*c*) depicts the contours of constant horizontal density gradient. In this figure the solid and dashed lines have density gradient values of ± 0.76 kg/m^4. Both figures 3(*b*) and 3(*c*) show the situation seven body oscillation periods after the start of the

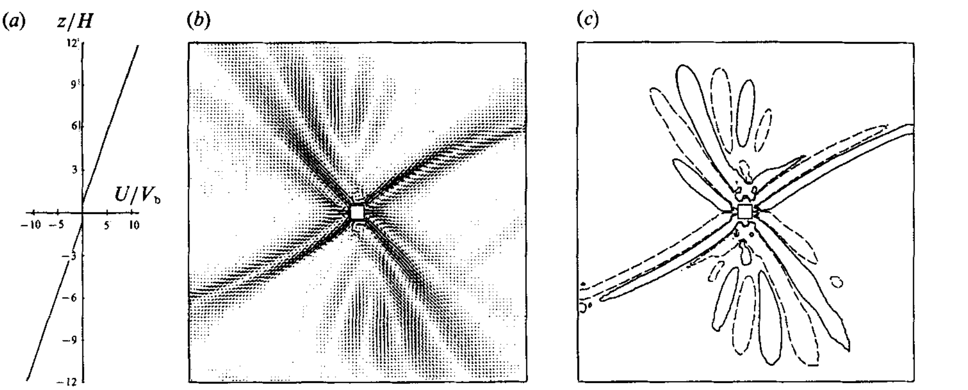

FIGURE 3. Finite-difference solution of the viscous cross-wave in a uniformly stratified linear shear layer. (*a*) Shear profile, the body height H is 20 mm and the maximum body velocity V_b is 0.785 mm/s. (*b*) Perturbation velocity vector plot. (*c*) Contours of constant horizontal density gradient: solid line is 0.76 kg/m^4 and the dashed line is -0.76 kg/m^4. Other conditions are the same as for figure 2.

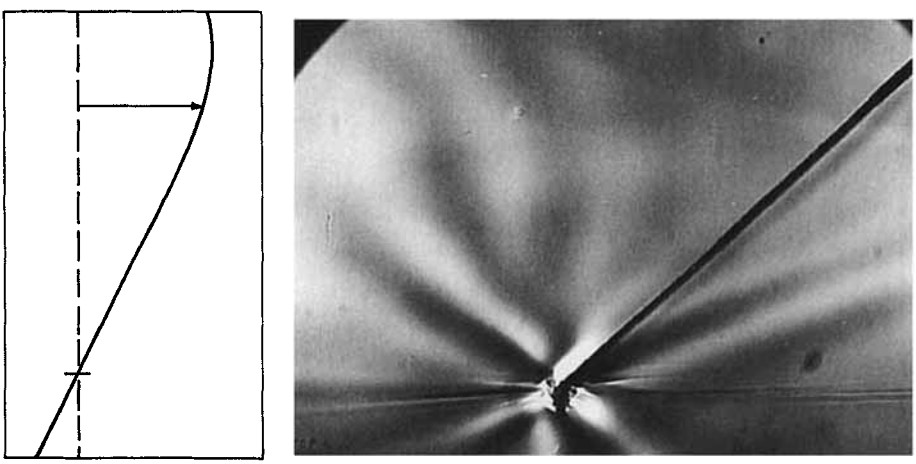

FIGURE 4. A schlieren photograph of a cross-wave. The conditions are close to those in figure 3.

oscillation. Internal wave energy which leaves the computational domain will not return and consequently the reflected waves should be slightly stronger than those predicted by the computations. The straight wave crests for energy propagating against the flow are shown by the finite-difference solution but there is a slight wave crest curvature in the energy moving with the flow. This is possibly due to the finite body size, or to the large wavenumber gradients being outside those acceptable for the WKB approximation, or simply that the region in the diagram is not the 'far-field' wave system evaluated in the analytical approach.

A notable absence of waves above the upper right arm and below the lower left arm of the cross in figure 3, unlike the predictions of figure 2 is primarily due to the damping effects of viscosity. Further towards the outer corners of these regions, waves are totally absent because energy that should have been there has reflection points outside the computational domain and is therefore lost.

In order to compare this theory with experiment a shear-flow tank has been used which has a working area of cross-section 0.3 m by 0.3 m. It has a pump with rotating

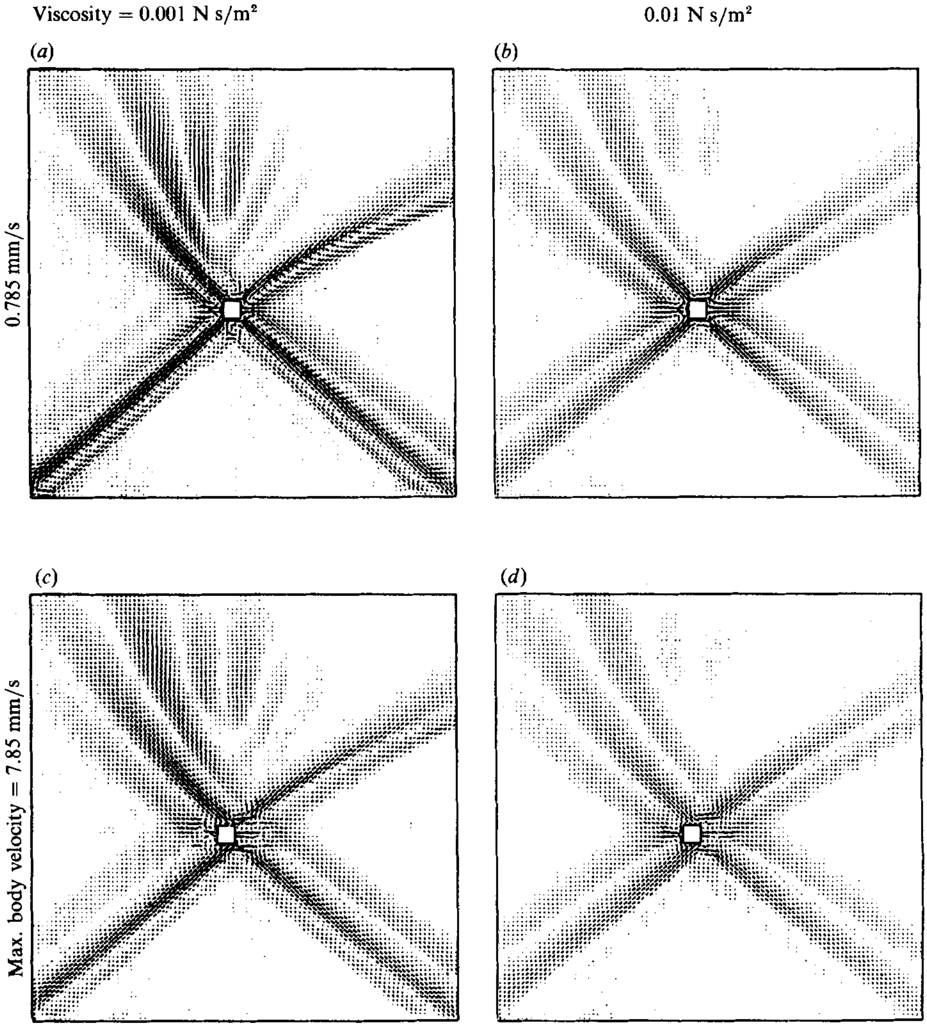

FIGURE 5. The effects of viscosity and amplitude of oscillation of the body on the wave in a linear shear. The shear is present only in the region above the body. The viscosity is 0.001 N s/m^2 for (*a*) and (*c*), and 0.01 N s/m^2 for (*b*) and (*d*). Other conditions are the same as for figure 3.

horizontal discs of the type described by Odell & Kovasznay (1971). The fluid travels 12 m in one circuit of the tank and the contraction ahead of the working section has an area ratio of 4:1. The fluid travels in one direction only and the shear is generated by graded gauzes downstream of the pump. A horizontal cylinder with a square cross-section is suspended from a trolley and moves at the same mean velocity as the fluid at the level of the cylinder. The cylinder is oscillated to produce the cross wave. Figure 4 shows a schlieren photograph of the wave system generated by the oscillating cylinder under similar conditions to those of figure 3. The horizontal cylinder has its axis normal to the flow which is from left to right in the photograph. We are looking along the length of the cylinder and the inclined black line in the photograph is the supporting strut.

The effects on the waves of the viscosity and the amplitude of oscillation of the body are illustrated in figures 5 and 6. The former shows the perturbation velocity vectors and the latter the contours of constant density perturbation. In these

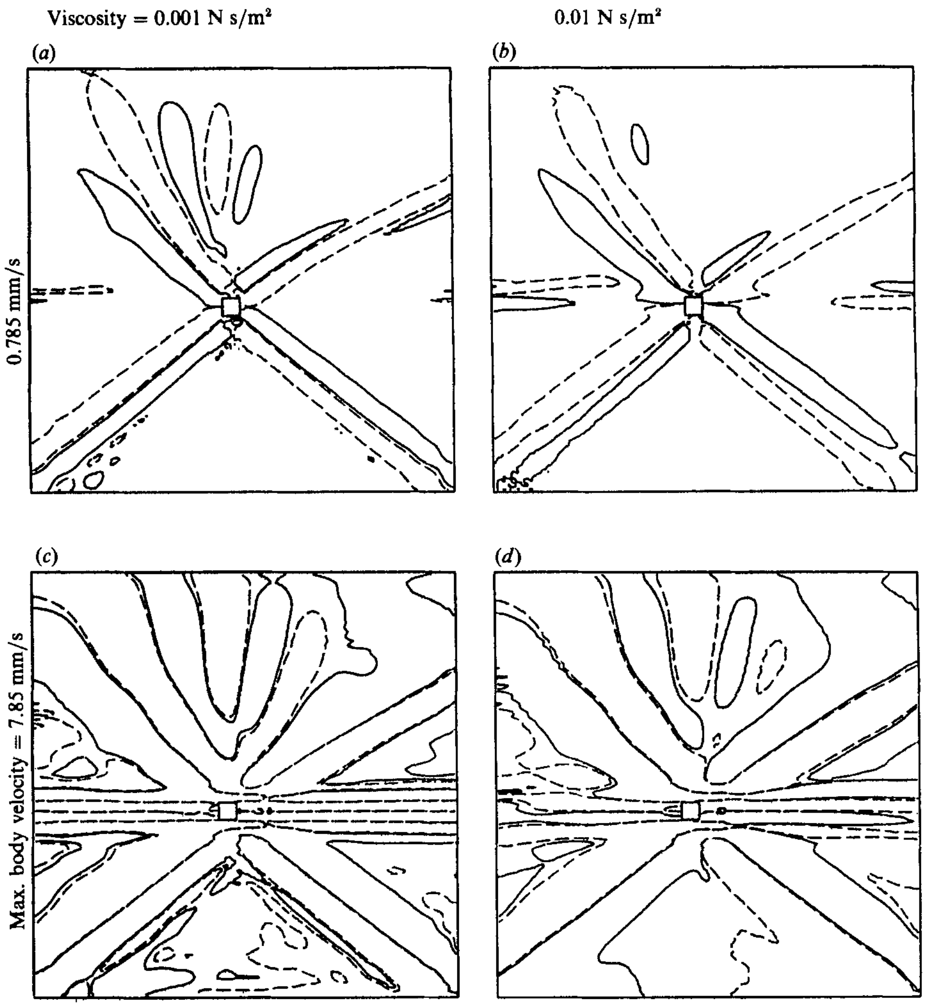

FIGURE 6. Contours of constant density perturbation corresponding to figure 5. The solid and dashed contours represent density perturbations of ± 0.009 kg/m^3.

calculations the background shear flow is present only in the region above the level of the body, so that the waves in the lower region of the computational domain are the usual viscous cross-waves. In figures 5 and 6, (*a*) and (*b*) correspond to a maximum body velocity of 0.785 mm/s whilst (*c*) and (*d*) have a maximum velocity of 7.85 mm/s. (*a*) and (*c*) have a viscosity of 0.001 N s/m^2, and (*b*) and (*d*) a viscosity of 0.01 N s/m^2. The velocities in each vector plot are made dimensionless by dividing by the maximum body velocity. The contours in figure 6 represent density perturbations of ± 0.009 kg/m^3 with the dashed lines corresponding to the negative value. As expected it is seen that an increase in viscosity reduces the amplitudes. When the amplitude of the body is increased the overall wave pattern remains unchanged except for the appearance of the wake on either side of the body.

Finally we consider the case of a linear shear layer overlying a region of stationary fluid with an oscillating body positioned some distance below in the stationary fluid. The attention is concentrated on the waves which will be propagating against the current after entering the shear layer. These waves will reflect at caustics in the shear

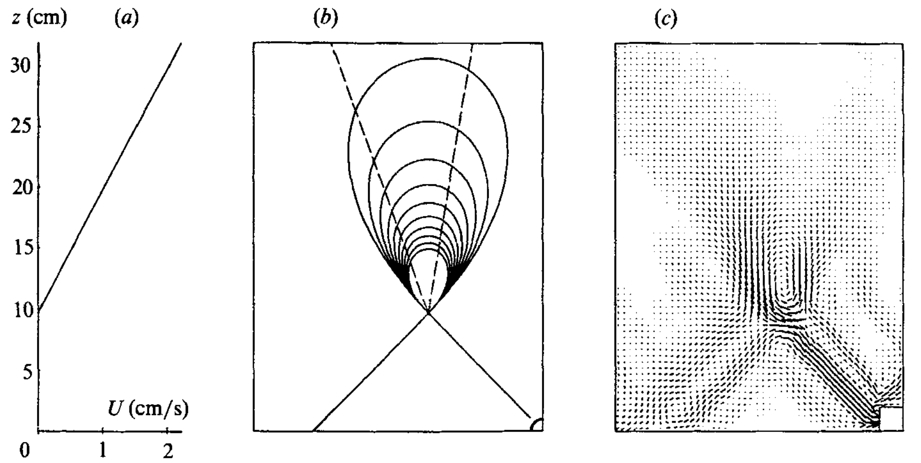

FIGURE 7. The cross-wave when the source is some distance below the shear flow in a region of stationary fluid. (*a*) The shear profile, $S = 0.1\ s^{-1}$. (*b*) The solid lines are ray paths and the dashed are lines of constant phase; the two dashed lines have the same phase. There are no further waves 2π apart. (*c*) Perturbation velocity vector plot, $N = 1.1$ rad/s, $\omega/N = 0.71$.

and will eventually return to the stationary fluid. Koop (1981, figure 10) presents a photograph of such waves. The photograph appears to confirm the point that wave reflections in shear flows are like those in a stationary thermocline, i.e. that they look like figure 1. Figure 7 (*b*) shows the ray pattern from the present calculations corresponding to the shear shown in figure 7 (*a*) and the conditions are similar to those in Koop's photograph. The corresponding finite-difference calculation is shown in figure 7 (*c*). It can be seen that at the most only two waves are present in the shear flow and these do not extend very far into the shear. With only two waves visible the overall wave pattern does look like that in a stationary thermocline but really the ray lines and phase configuration are fundamentally different.

In general in wave systems the ray lines are different from the lines of constant phase. It is the waves from a simple harmonic oscillation in a thermocline that are the exception, with ray lines and the phase configuration coincident.

In this paper ray theory has been used to develop equations for the phase configurations around an oscillatory disturbance in a stratified shear flow. For the special case when the shear is linear, the wave crests are straight lines passing through the source. The analytical results have been supported by experiment and by finite-difference calculations of internal waves under similar conditions. The numerical results show regions where the lines of constant phase are slightly curved. This is probably due to the finite body size and to the large wavenumber gradients being outside those acceptable for the WKB approximation which was used for the analytical solution.

The work was supported by the Admiralty Research Establishment, Ministry of Defence.

REFERENCES

APPLEBY, J. C. & CRIGHTON, D. G. 1986 Non-Boussinesq effects in the diffraction of internal waves from an oscillating cylinder. *Q. J. Mech. Appl. Maths* **39**, 209.

APPLEBY, J. C. & CRIGHTON, D. G. 1987 Internal gravity waves generated by oscillations of a sphere. *J. Fluid Mech.* **183**, 439.

BOOKER, J. R. & BRETHERTON, F. P. 1967 The critical layer for internal gravity waves in a shear flow. *J. Fluid Mech.* **27**, 513.

BRETHERTON, F. P. 1966 The propagation of groups of internal waves in a shear flow. *Q. J. Roy. Met. Soc.* **92**, 466.

GORDON, D., KLEMENT, U. R. & STEVENSON, T. N. 1975 A viscous internal wave in a stratified fluid whose buoyancy frequency varies with altitude. *J. Fluid Mech.* **69**, 615.

GORDON, D. & STEVENSON, T. N. 1972 Viscous effects in a vertically propagating internal wave. *J. Fluid Mech.* **56**, 629.

GRIMSHAW, R. 1974 Internal gravity waves in a slowly varying dissipative medium. *Geophys. Fluid Dyn.* **6**, 131.

HIRT, C. W. & COOK, J. L. 1972 Calculating three dimensional flows around structures and over rough terrain. *J. Comput. Phys.* **10**, 324.

KOOP, C. G. 1981 A preliminary investigation of the interaction of internal gravity waves with a steady shearing motion. *J. Fluid Mech.* **113**, 347.

KOOP, C. G. & MCGEE, B. 1986 Measurements of internal gravity waves in a continuously stratified shear flow. *J. Fluid Mech.* **172**, 453.

LIGHTHILL, M. J. 1978 *Waves in Fluids*. Cambridge University Press.

LIU, R. 1989 A numerical and analytical study of internal waves in stratified fluids. Ph.D. thesis, University of Manchester.

LIU, R. & STEVENSON, T. N. 1989 A finite difference method for modelling internal waves. *Aero Rep.* 8908. Dept of Engng, University of Manchester.

MOWBRAY, D. E. & RARITY, B. S. H. 1967 A theoretical and experimental investigation of the phase configuration of internal waves of small amplitude in a density stratified liquid. *J. Fluid Mech.* **28**, 1.

ODELL, G. M. & KOVASZNAY, L. S. G. 1971 A new type of water channel with density stratification. *J. Fluid Mech.* **50**, 535.

PHILLIPS, O. M. 1966 *The Dynamics of the Upper Ocean*. Cambridge University Press.

THOMAS, N. H. & STEVENSON, T. N. 1972 A similarity solution for viscous internal waves. *J. Fluid Mech.* **54**, 495.

YOUNG, J. A. & HIRT, C. W. 1972 Numerical calculation of internal wave motions. *J. Fluid Mech.* **56**, 265.